

Proactive Routing to Interpretable Surrogates with Distribution-Free Safety Guarantees

Iqtedar Uddin
Illinois Institute of Technology
iuddin1@hawk.illinoistech.edu

Mazin Khider
Illinois Institute of Technology
mkhider@hawk.illinoistech.edu

André Bauer
Illinois Institute of Technology
abauer7@illinoistech.edu

Abstract

Model routing determines whether to use an accurate black-box model or a simpler surrogate that approximates it at lower cost or greater interpretability. In deployment settings, practitioners often wish to restrict surrogate use to inputs where its degradation relative to a reference model is controlled. We study proactive (input-based) routing, in which a lightweight gate selects the model before either runs, enabling distribution-free control of the fraction of routed inputs whose degradation exceeds a tolerance τ . The gate is trained to distinguish safe from unsafe inputs, and a routing threshold is chosen via Clopper–Pearson conformal calibration on a held-out set, guaranteeing that the routed-set violation rate is at most α with probability $1 - \delta$. We derive a feasibility condition linking safe routing to the base safe rate π and risk budget α , along with sufficient AUC thresholds ensuring that feasible routing exists. Across 35 OpenML datasets and multiple black-box model families, gate-based conformal routing maintains controlled violation while achieving substantially higher coverage than regression conformal and naive baselines. We further show that probabilistic calibration primarily affects routing efficiency rather than distribution-free validity.

1 Introduction

Practitioners increasingly face a deployment dilemma: interpretable models such as shallow decision trees and linear regressors are auditable, fast, and regulatorily favored, but are rejected in favor of black-box ensembles because no formal mechanism exists to establish when they are accurate enough to use. The intuitive solution—deploy the interpretable model when it agrees with the black-box, i.e., when $|f(x) - g(x)| \leq \tau$ —requires running the expensive model on every input, defeating the purpose. We propose a proactive solution: identify safe inputs from features alone, before either model runs, with formal guarantees on the fraction of routed inputs where quality degrades unacceptably. When the interpretable surrogate performs acceptably on a given input, using it saves substantial compute with negligible quality loss. Local explanation methods such as LIME [Ribeiro et al., 2016] and SHAP [Lundberg and Lee, 2017] construct surrogates to approximate black-box behavior. Our framework shows when such surrogates can safely replace the black-box rather than merely explain it, addressing the practical tension between black-box accuracy and interpretable deployment emphasized by Rudin [Rudin, 2019].

Model routing formalizes this choice: given an expensive model f and a cheap surrogate g , decide per-input x which to use. Existing approaches include cascading [Viola and Jones, 2001, Trapeznikov

and Saligrama, 2013, Chen et al., 2023], where the cheap model runs first and escalates to the expensive model if uncertain, and disagreement routing [Ribeiro et al., 2016], where the surrogate is used when $|f(x) - g(x)| \leq \tau$. Both approaches are output-dependent. They require running at least one model before deciding. Cascading must run g on every input. Disagreement routing requires $f(x)$, largely defeating the purpose of cost savings. Furthermore, while some frameworks utilize input-based routing to dynamically skip computation for efficiency [Wang et al., 2018, Wu et al., 2018], they rely on empirical heuristics and do not provide formal guarantees on the quality of the routed predictions.

We propose proactive routing with distribution-free safety guarantees. A lightweight classifier we call the *gate* maps input features to a safety score $s : \mathcal{X} \rightarrow [0, 1]$ before either model runs. Unlike cascading, where the cheap model must process every input before deciding to escalate, and unlike disagreement routing, where the expensive model’s output $f(x)$ is needed, our gate examines only the input x and makes an immediate routing decision.

The gate is trained to distinguish inputs where the surrogate performs acceptably (degradation $d(x) \leq \tau$) from those where it does not. A conformal calibration procedure then selects a routing threshold t^* from a held-out calibration set, providing a PAC-style guarantee:

$$\Pr\left(\Pr(d(X) > \tau \mid s(X) \geq t^*) > \alpha\right) \leq \delta.$$

This guarantee is distribution-free, requiring only exchangeability between calibration and test data. It holds regardless of the gate’s calibration quality (ECE) [Guo et al., 2017], model family, or data distribution.

Contributions. We formalize proactive surrogate routing and derive an exact finite-sample bound on routed-set violation via Clopper–Pearson conformal calibration. We characterize routing feasibility through a likelihood-ratio condition and sufficient AUC thresholds, and establish a tight lower bound on achievable coverage under concavity. We show that distribution-free validity is independent of probabilistic calibration, though calibration affects efficiency. Empirically, across diverse tabular benchmarks (LCBench and OpenML), gate conformal routing achieves higher coverage with controlled violations compared to regression-based baselines.

2 Related Work

Conformal prediction and risk control. Split conformal prediction [Vovk et al., 2005] constructs distribution-free prediction sets with finite-sample coverage guarantees. Conformal Risk Control [Bates et al., 2021] guarantees $\mathbb{E}[L(\lambda)] \leq \alpha$, controlling expected loss. Our framework provides a stronger high-probability guarantee: $\Pr(V(t^*) > \alpha) \leq \delta$, bounding the probability of any exceedance. Expected risk control permits frequent violations on individual deployments. Our guarantee ensures that the violation rate exceeds α with probability at most δ , which is the relevant requirement for safety-critical deployment. Learn Then Test [Angelopoulos et al., 2022] provides a comparable high-probability guarantee over families of thresholds. Our Clopper–Pearson approach achieves the same guarantee type for nested thresholds with a simpler mechanism, justified by the fixed-sequence testing argument (Remark 1).

Selective prediction and deferral. The reject option [Chow, 1970, El-Yaniv and Wiener, 2010] allows classifiers to abstain on uncertain inputs, trading coverage for accuracy. Selective classification [Geifman and El-Yaniv, 2017] provides risk-coverage tradeoffs for deep networks. Learning to

defer [Madras et al., 2018] routes inputs to human experts. Our framework generalizes selective prediction: rather than abstaining (discarding the input), we route to an alternative model. The safety constraint is on substitution quality, not prediction correctness. While selective classification controls conditional accuracy above a confidence threshold, we instead control degradation relative to a reference model and replace abstention with an alternative predictor. Although the conditional risk bound has a similar mathematical form, our safety criterion measures surrogate degradation rather than prediction correctness alone.

Model cascading and routing. Cascades [Viola and Jones, 2001, Trapeznikov and Saligrama, 2013] run models sequentially, escalating when confidence is low. FrugalGPT [Chen et al., 2023] and Hybrid LLM [Ding et al., 2024] cascade through LLM APIs. Mixture-of-experts [Jacobs et al., 1991] routes via learned gating networks. These approaches are largely output-dependent: routing decisions use model outputs (confidence, predictions). Conversely, input-based routing frameworks [Wang et al., 2018, Wu et al., 2018] dynamically skip computation by evaluating only the input features x before the main models run, reducing latency and avoiding unnecessary computation on the cheap model for hard inputs. However, these proactive methods rely on empirical heuristics and lack formal guarantees on prediction quality. While an input-based gate requires labeled training data from both models, this is a one-time offline cost amortized over all future inference.

Recent works on model selection with guarantees have successfully addressed prediction quality, but primarily through output-dependent approaches: post-hoc arbiters Overman and Bayati [2025], output-based selective prediction Wang et al. [2026], Valkanas et al. [2025], and guaranteed sequential cascades Chen et al. [2023]. Because these methods require executing at least one model before making routing decisions, they incur the very computational cost proactive routing aims to avoid. By framing proactive routing as an input-only classification task governed by a Neyman–Pearson feasibility condition, we characterize its theoretical limits and provide exact finite-sample safety bounds on the routed subset without requiring prior model execution.

Surrogate fidelity and interpretability. LIME [Ribeiro et al., 2016] and SHAP [Lundberg and Lee, 2017] construct local surrogates to explain black-box predictions, routing implicitly when the surrogate agrees with the black-box (fidelity-based, i.e., $|f(x) - g(x)| \leq \tau$). This requires $f(x)$, which defeats proactive routing. Rudin [Rudin, 2019] argues that practitioners default to black-boxes precisely because interpretable models lack formal per-instance deployment guarantees. Knowledge distillation [Hinton et al., 2015] trains surrogates globally but provides no such guarantee. We close this gap: our safety criterion is degradation relative to ground truth rather than agreement with the black-box, ensuring the surrogate is genuinely accurate on routed inputs—providing a formal safety characterization that complements Rudin’s call for interpretable models in high-stakes settings.

Calibration. Modern neural networks are often miscalibrated [Guo et al., 2017]. Post-hoc methods, including Platt scaling [Niculescu-Mizil and Caruana, 2005] and beta calibration [Kull et al., 2017], are commonly used to align predicted probabilities with true empirical frequencies. In our framework, probabilistic calibration is not strictly required for theoretical validity. The conformal procedure provides distribution-free safety guarantees regardless of the gate’s Expected Calibration Error (ECE). However, we demonstrate empirically that correcting overconfident or underconfident gates via these methods affects threshold dynamics. Better calibration prevents the conformal procedure from selecting extreme thresholds to compensate for skewed score distributions. Recalibration may increase or decrease raw coverage depending on the initial miscalibration direction. However, it produces a more stable violation rate in finite-sample settings.

3 Problem Formulation

Let $f : \mathcal{X} \rightarrow \mathbb{R}$ be an accurate black-box model and $g : \mathcal{X} \rightarrow \mathbb{R}$ a simpler surrogate. Given input x with true label y , we define the degradation:

$$d(x, y) = |y - g(x)| - |y - f(x)|, \quad (1)$$

which is the increase in absolute error from using g instead of f . Positive d means the surrogate is worse, and negative d means it is better. Given tolerance $\tau \in \mathbb{R}$, an input is *safe* if $d(x, y) \leq \tau$:

$$Y(x) = \mathbf{1}[d(x, y) \leq \tau], \quad \pi = \Pr(Y = 1). \quad (2)$$

A routing policy $\hat{\pi}(x) = \mathbf{1}[s(x) \geq t]$ routes to the surrogate when gate score $s(x)$ exceeds threshold t . The *violation rate* among routed inputs is:

$$\begin{aligned} V(t) &= \Pr(Y = 0 \mid s(X) \geq t) \\ &= \frac{(1 - \pi) \text{FPR}(t)}{(1 - \pi) \text{FPR}(t) + \pi \text{TPR}(t)}, \end{aligned} \quad (3)$$

where $\text{TPR}(t) = \Pr(s(X) \geq t \mid Y = 1)$ and $\text{FPR}(t) = \Pr(s(X) \geq t \mid Y = 0)$.

Note that computing degradation labels requires running both f and g on the training and calibration sets. This is a one-time offline cost.

Definition 1 (Safe routing problem). *Find threshold t maximizing coverage $\Pr(s(X) \geq t)$ subject to $V(t) \leq \alpha$.*

The parameters τ and α are decoupled: τ defines what “safe” means (continuous tolerance), while α controls what fraction of violations is acceptable among routed inputs. Setting $\tau = 1.0, \alpha = 0.2$ means: among inputs routed to the surrogate, at most 20% may have degradation exceeding 1.0 units.

While we instantiate safety via degradation relative to the expensive model, the framework applies to any measurable objective that induces a binary safety label, including fidelity-based criteria or application-specific utility functions.

4 Method

4.1 Gate Training

We train a logistic regression classifier to predict Y from input features x . The gate outputs $s(x) = \hat{p}(Y = 1|x)$, optionally calibrated via Platt scaling (also known as sigmoid calibration) [Platt, 1999, Niculescu-Mizil and Caruana, 2005] using a cross-validated holdout set. We use logistic regression as the gate classifier to minimize computational overhead. As a lightweight, linear baseline, it demonstrates that our conformal framework provides safe and efficient routing without requiring a complex, computationally expensive gate. Logistic regression also yields scores that are monotone in the likelihood ratio, producing concave ROC curves in the population limit [Fawcett, 2006]. This activates the tighter feasibility bound of Theorem 2 and the coverage bound of Theorem 3.

4.2 Conformal Threshold Selection

Following the framework of Conformal Risk Control [Angelopoulos and Bates, 2022, Bates et al., 2021], we use a calibration set $\{(s_i, Y_i)\}_{i=1}^n$ independent of training and test data to select the optimal routing threshold. Specifically, we select t^* as the lowest threshold where the Clopper–Pearson [Clopper and Pearson, 1934] upper confidence bound on the violation rate is at most α :

$$t^* = \min \left\{ t \in \{s_1, \dots, s_n\} : \text{UCB}_\delta(k(t), n(t)) \leq \alpha \right\}, \quad (4)$$

where $n(t) = |\{i : s_i \geq t\}|$, $k(t) = |\{i : s_i \geq t, Y_i = 0\}|$, and

$$\text{UCB}_\delta(k, n) = B^{-1}(1 - \delta; k + 1, n - k) \quad (5)$$

is the exact one-sided Clopper–Pearson upper bound, with B^{-1} the Beta quantile function. If no valid t exists, $t^* = \infty$ (route nothing).

Proposition 1 (Finite-sample guarantee). *For any gate s , any distribution over (X, Y) , and calibration set of size n exchangeable with the test point:*

$$\Pr(V(t^*) > \alpha) \leq \delta.$$

This follows directly from the coverage property of the Clopper–Pearson interval [Clopper and Pearson, 1934]: $\Pr(\hat{p} \leq \text{UCB}_\delta(k, n)) \geq 1 - \delta$ for any true proportion \hat{p} , where $k \sim \text{Binomial}(n, \hat{p})$. With $n \approx 300$ calibration points (our setup), the bound is tight: for $k = 0$ unsafe among $n = 300$ routed calibration points, $\text{UCB}_{0.10}(0, 300) = 0.0076$, enabling routing with α as low as 0.01.

Algorithm 1 Conformal Gate Routing

Require: Calibration scores $\{s_i\}_{i=1}^n$, labels $\{Y_i\}_{i=1}^n$, risk α , confidence δ

- 1: Sort unique scores: $t_1 < t_2 < \dots < t_m$
 - 2: **for** $j = 1, \dots, m$ **do**
 - 3: $n_j \leftarrow |\{i : s_i \geq t_j\}|$, $k_j \leftarrow |\{i : s_i \geq t_j, Y_i = 0\}|$
 - 4: **if** $\text{UCB}_\delta(k_j, n_j) \leq \alpha$ **then**
 - 5: **return** $t^* = t_j$
 - 6: **end if**
 - 7: **end for**
 - 8: **return** $t^* = \infty$ {Abstain from routing}
-

Remark 1 (Validity under threshold search). *Algorithm 1 evaluates multiple candidate thresholds on the same calibration data. We now argue that post-selection validity holds without any multiplicity correction. Condition on the realized gate scores $\{s_i\}_{i=1}^n$. The threshold ordering $t_1 < t_2 < \dots < t_m$ is then deterministic, and the routed sets $\{i : s_i \geq t_j\}$ are fixed. The safety labels $\{Y_i\}_{i=1}^n$ depend on (x_i, y_i) and the pre-trained models f and g . Because the gate is trained on a separate split, these labels remain exchangeable conditional on the scores. Each Clopper–Pearson test is therefore exact given the scores. Algorithm 1 tests thresholds in a fixed ascending order and accepts the first one satisfying $\text{UCB}_\delta(k_j, n_j) \leq \alpha$. By the fixed-sequence testing principle [Marcus et al., 1976], this controls the family-wise error rate at level δ . The unconditional guarantee $\Pr(V(t^*) > \alpha) \leq \delta$ follows by iterated expectation. No Bonferroni correction or alternative calibration framework is required.*

5 Theoretical Analysis

5.1 Routing Feasibility

Proposition 2 (Feasibility condition). *The constraint $V(t) \leq \alpha$ is satisfiable with positive coverage if and only if there exists threshold t such that:*

$$\frac{\text{TPR}(t)}{\text{FPR}(t)} \geq C(\pi, \alpha) \triangleq \frac{(1 - \pi)(1 - \alpha)}{\pi\alpha}. \quad (6)$$

The full algebraic derivation appears in Appendix A.

Remark on Optimality. Condition (6) implies that for any fixed false positive rate, the violation rate is minimized by maximizing the True Positive Rate. By the Neyman–Pearson lemma [Neyman and Pearson, 1933], the likelihood ratio test is the most powerful test for this objective. Thus, the optimal gate $s(x)$ is the likelihood ratio $P(Y = 1|x)/P(Y = 0|x)$, which monotonically maps to the posterior $P(Y = 1|x)$ used in our experiments.

The critical ratio $C(\pi, \alpha)$ captures the interaction between τ (via π) and the risk budget α . When π is large (lenient τ , most inputs safe), C is small and even weak gates suffice. When π is small (strict τ), C grows and only gates with strong separation can route safely.

Following standard geometric formulations of Receiver Operating Characteristic (ROC) analysis [Fawcett, 2006], we can translate this likelihood-ratio condition directly into ROC space.

Corollary 1 (ROC Feasibility Geometry). *Let*

$$C(\pi, \alpha) = \frac{(1 - \pi)(1 - \alpha)}{\pi\alpha}.$$

Feasible routing exists if and only if the ROC curve intersects the half-space

$$\{(u, v) \in [0, 1]^2 : v \geq C(\pi, \alpha)u\}.$$

Equivalently, there exists a threshold t such that $\text{TPR}(t) \geq C(\pi, \alpha)\text{FPR}(t)$.

The full algebraic derivation appears in Appendix A.

5.2 Critical AUC

Theorem 1 (Sufficient AUC for feasibility). *Define the critical AUC:*

$$\Phi_c(\pi, \alpha) = \min\left(1, \frac{C(\pi, \alpha)}{2}\right). \quad (7)$$

If $\text{AUC} \geq \Phi_c(\pi, \alpha)$, then there exists a routing threshold t satisfying $V(t) \leq \alpha$ with positive coverage.

The full algebraic derivation appears in Appendix A.

Remark 2. *Theorem 1 is sufficient but conservative. Theorem 2 partially closes the gap: at $\tau = 0.5$, the required AUC drops from $\Phi_c = 1.0$ to $\Phi_c^* = 0.76$. The residual gap (observed AUC $0.57 < 0.76$, yet routing succeeds) reflects a fundamental limit of scalar summaries: feasibility is a local ROC property (Corollary 1), while AUC is global. No single-scalar condition can be both necessary and sufficient. This yields a hierarchy: Corollary 1 (exact, requires full ROC) \rightarrow Theorem 2 (tight scalar, concave ROC) \rightarrow Theorem 1 (sufficient, any ROC).*

Corollary 2. As $\alpha \rightarrow 0$ or $\pi \rightarrow 0$: $\Phi_c \rightarrow 1$, so near-perfect ranking is required. For $\pi = 0.82$ (our $\tau = 2.0$) and $\alpha = 0.2$, we have $C = 0.88$ and $\Phi_c = 0.44$. Our observed AUC of 0.59 exceeds this threshold, confirming feasibility. For $\pi = 0.66$ ($\tau = 0.5$) and $\alpha = 0.2$: $\Phi_c = 1.0$ but $\Phi_c^* = 0.76$ (Theorem 2), yet routing succeeds empirically with 24% coverage, illustrating that even the tight bound cannot capture local ROC structure.

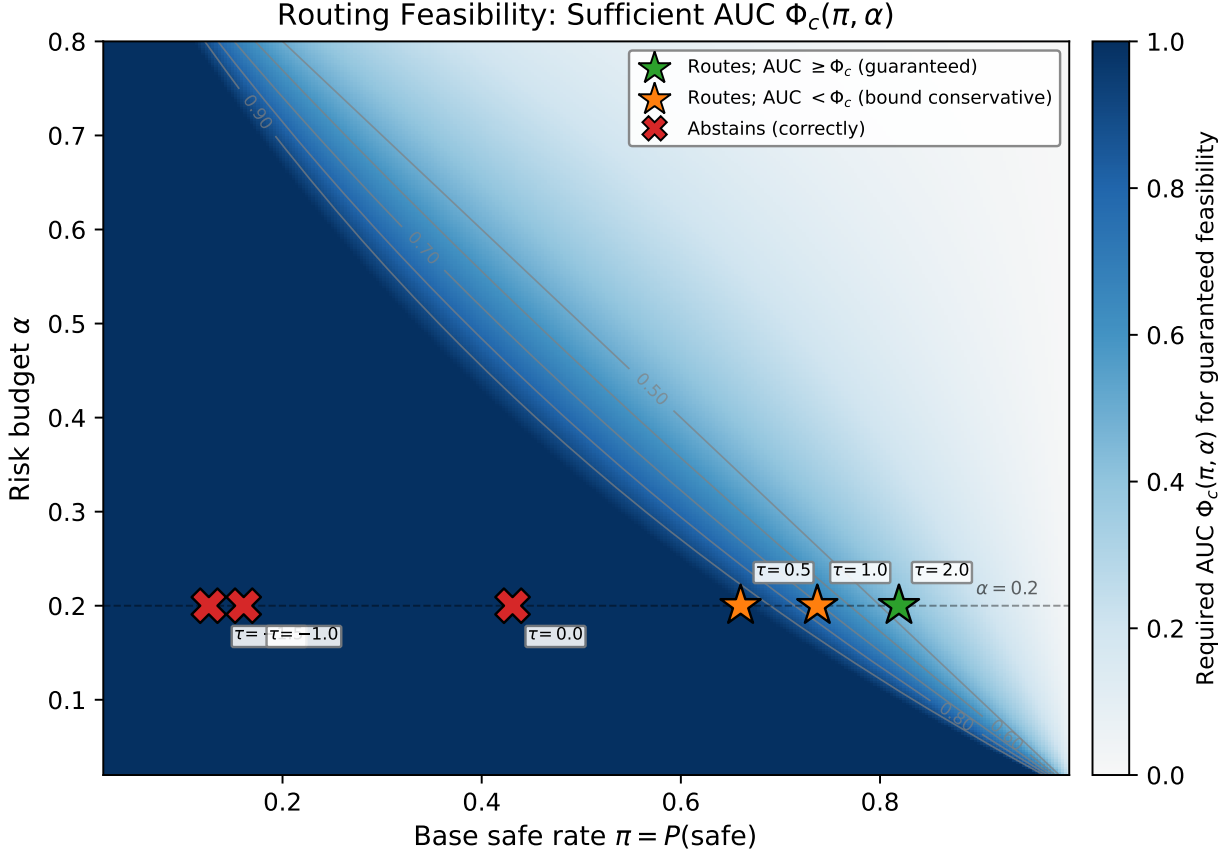


Figure 1: Feasibility landscape: critical AUC $\Phi_c(\pi, \alpha)$ as a function of base safe rate π and risk budget α . Darker regions require higher AUC for guaranteed feasibility. Stars mark our six τ operating points at $\alpha = 0.2$, colored by empirical outcome: green if routing achieves positive coverage, red if coverage is zero. At $\tau \leq 0$ (low π), the gate falls in the hard region and correctly abstains. At $\tau = 0.5$ and $\tau = 1.0$, routing succeeds despite AUC falling below Φ_c , illustrating that the sufficient condition is conservative. At $\tau = 2.0$, AUC exceeds Φ_c and feasibility is guaranteed.

Theorem 2 (Tight AUC under concavity). Let $C = C(\pi, \alpha)$. For any gate with concave ROC curve, define

$$\Phi_c^*(\pi, \alpha) = \begin{cases} 1 - \frac{1}{2C} & \text{if } C > 1, \\ \frac{1}{2} & \text{if } C \leq 1. \end{cases} \quad (8)$$

- (i) If $\text{AUC} \geq \Phi_c^*$, feasible routing exists.
- (ii) The bound is tight: for any $\varepsilon > 0$, a concave ROC with $\text{AUC} = \Phi_c^* - \varepsilon$ exists that is infeasible.

(iii) $\Phi_c^* < \Phi_c$ for all $C > 1$, strictly improving Theorem 1.

The full algebraic derivation appears in Appendix A.

Theorem 3 (Coverage bound). *Under the conditions of Theorem 2 with $C > 1$ and $\text{AUC} = A \geq \Phi_c^*$, the optimal coverage subject to $V(t) \leq \alpha$ satisfies $\text{Cov}^* \geq \min\{1, (2A - 1)(1 - \pi)/[(C - 1)\alpha]\}$. The bound is tight (Appendix B.2).*

5.3 The Calibration–Efficiency Separation

The conformal guarantee (Proposition 1) holds for any gate score $s(x)$, independent of its probabilistic calibration. However, calibration affects efficiency (coverage) and the finite-sample stability of the selected threshold.

For a perfectly calibrated gate with $s(x) = \Pr(Y = 1 | x)$, the expected violation rate at threshold t equals $1 - t$, so the conformal procedure selects $t^* \approx 1 - \alpha$ (up to finite-sample correction). If the gate is overconfident (e.g., $s(x) = 0.9$ when the true probability is 0.7), conformal compensates by shifting to a more extreme threshold (e.g., $t^* = 0.95$). Underconfidence similarly forces lower thresholds. In all cases safety is preserved, but extreme thresholds increase sensitivity to finite-sample noise, leading to higher variance in realized violations.

Thus, calibration determines which inputs are routed, how many are routed, and threshold stability, but not the validity of the risk bound. Appendix E confirms this empirically: beta calibration [Kull et al., 2017], temperature scaling [Guo et al., 2017], and isotonic regression [Zadrozny and Elkan, 2002] reduce ECE (0.18 to 0.06) while preserving safety. Coverage changes only marginally ($\leq 2.5\text{pp}$). Overall efficiency remains primarily governed by ranking quality (AUC), while calibration stabilizes finite-sample thresholding.

6 Experiments

6.1 Setup

We evaluate our approach on 35 regression datasets from LCBench [Zimmer et al., 2021, Vanschoren et al., 2014], where each dataset corresponds to a different OpenML classification task and contains 2000 hyperparameter configurations with recorded validation accuracy at epoch 50. Inputs are hyperparameter settings (learning rate, batch size, architecture choices, etc.) and the target is validation accuracy. Data is split 55/15/15/15 into train, validation, calibration, and test sets with strict separation. Additional experiments on 22 general-purpose OpenML regression datasets (air quality, housing, energy, chemistry, physics, robotics, etc.) are reported in Appendix F.

The expensive model f is a random forest [Breiman, 2001], treated as a black-box ensemble with 1500 trees. The cheap surrogate g is a decision tree with depth selected on the validation set from $\{2, 3, 4, 5, 7, 9, 11, 13, 15\}$ by minimizing MAE. Degradation is $d(x) = |y - g(x)| - |y - f(x)|$.

We evaluate six tolerance levels $\tau \in \{-1.5, -1.0, 0.0, 0.5, 1.0, 2.0\}$ spanning strict ($\tau < 0$: surrogate must be better) to lenient ($\tau = 2.0$: up to 2.0 extra error acceptable). We test ten risk levels $\alpha \in \{0.05, 0.10, \dots, 0.80\}$ with $\delta = 0.10$.

6.2 Methods

We compare against five baselines:

1. **Gate conformal** (ours): logistic regression gate with Clopper–Pearson threshold selection.

2. **Naive** ($t = 0.5$): route if gate score ≥ 0.5 . No formal guarantee.
3. **Oracle**: route iff $d(x) \leq \tau$. This provides an upper bound on achievable coverage.
4. **Always-BB / Always-CM**: never/always route.
5. **Random (matched)**: route uniformly at random at conformal’s coverage level.
6. **Regression Conformal (Baseline)**: As an alternative to the binary gate, we predict the degradation $d(x)$ via regression. We train a ridge model [Hoerl and Kennard, 1970] $\hat{h}(x)$ and apply split conformal regression [Papadopoulos et al., 2002, Lei et al., 2018] to obtain an upper bound $\hat{d}_{\text{UCB}}(x)$ at level $1 - \alpha$, routing when $\hat{d}_{\text{UCB}}(x) \leq \tau$. A non-linear `HistGradientBoostingRegressor` yields similar results (Appendix E.1), indicating the gap is not driven by regressor capacity.

6.3 Gate Properties, Feasibility, and Guarantee Reliability

Table 1: Gate properties across tolerance levels. π : base safe rate; AUC: gate ranking quality (median [IQR]); ECE: calibration error. Φ_c/Φ_c^* : sufficient AUC thresholds from Theorems 1/2. Coverage and mean violation at $\alpha = 0.2$ averaged over 35 datasets.

τ	π	AUC (med.)	ECE	Φ_c	Φ_c^*	Conf. ($\alpha=0.2$)	
						Cov.	Viol.
-1.5	0.13	0.71	0.07	1.00	0.92	0.000	—
-1.0	0.16	0.70	0.09	1.00	0.95	0.000	—
0.0	0.43	0.54	0.25	1.00	0.88	0.003	0.03
0.5	0.66	0.57	0.20	1.00	0.76	0.243	0.15
1.0	0.74	0.58	0.17	0.70	0.65	0.446	0.14
2.0	0.82	0.59	0.12	0.44	0.50	0.661	0.12

Table 2: Fraction of (dataset, τ) pairs where the realized violation rate exceeds target α . Gate conformal is broadly consistent with $\delta = 0.10$. Baselines violate substantially more often.

α	Gate Conf.		Reg. Conf.		Naive	
0.10	7/34	(21%)	31/50	(62%)	151/172	(88%)
0.20	8/66	(12%)	57/102	(56%)	128/172	(74%)
0.30	6/82	(7%)	80/144	(56%)	106/172	(62%)
0.50	8/112	(7%)	64/181	(35%)	62/172	(36%)

Tables 1–2 summarize (i) when routing is feasible (Proposition 2) and (ii) how often the target is met across datasets.

π drives feasibility (ROC geometry). At $\tau \leq 0$, $\pi < 0.45$ and the sufficient bound gives $\Phi_c = 1.0$, so the conformal procedure abstains (zero coverage), consistent with Proposition 2. At $\tau \geq 1.0$, π increases ($\pi \geq 0.74$), reducing the required separation (smaller $C(\pi, \alpha)$) and enabling substantial coverage (e.g., 66% at $\tau = 2.0$).

Moderate AUC can suffice due to local ROC slope. Although Theorems 1–2 provide useful scalar feasibility thresholds, feasibility is ultimately a local ROC condition: the conformal search can select a threshold that isolates a small, high-purity region (steep initial ROC slope) even when global AUC is modest. This explains successful routing at $\tau \in \{0.5, 1.0\}$ despite AUC falling below Φ_c .

ECE affects efficiency, not validity. ECE varies widely (0.07–0.25) and peaks near $\tau = 0$ where the task is most ambiguous, but the distribution-free guarantee depends only on the calibration procedure, not on probabilistic calibration quality (Section 5.3). Miscalibration primarily shifts the selected threshold t^* and thus coverage, rather than invalidating the risk control.

Guarantee reliability across datasets. Table 2 is the main empirical validity check. Gate conformal exceeds α on 7–12% of (dataset, τ) pairs for $\alpha \geq 0.2$. This is broadly consistent with $\delta = 0.10$. At $\alpha = 0.10$, the exceedance rate rises to 21%. This occurs because at strict α , the conformal procedure selects high thresholds that route very few calibration points. When the effective routed calibration size $n(t^*)$ is small, the CP bound is correct but necessarily loose. The denominator of (dataset, τ) pairs achieving positive coverage is also dominated by borderline-feasible settings at this strict level. For $\alpha \geq 0.20$, routed calibration sets are larger and exceedance rates (7–12%) align with the nominal $\delta = 0.10$. In contrast, regression conformal and naive thresholding violate α on 35–88% of cases. This indicates that direct regression on degradation is substantially less reliable for conditional risk control.

Robustness to model families. We replicate the evaluation with XGBoost [Chen and Guestrin, 2016] and MLP [Goodfellow et al., 2016] as the expensive model (same decision-tree surrogate). Qualitative conclusions remain unchanged. Full results appear in Appendices D–E.

6.4 Coverage–Violation Pareto Frontier

Figure 2 shows the empirical Pareto frontier characterizing the standard risk-coverage tradeoff [El-Yaniv and Wiener, 2010] at $\alpha = 0.2$. Gate conformal traces a frontier consistently below the α line, reaching 66% coverage at $\tau = 2.0$ with only 12% mean violation. Regression conformal achieves lower coverage (58%) at higher violation (15%), and naive thresholding violates α at every operating point. Gate conformal dominates on both axes at all practical τ values (≥ 0.5).

At low τ , regression conformal routes a tiny fraction (0.1–3%) with massive violation (8–51%), while gate conformal correctly abstains. This illustrates the value of the conformal abstention mechanism: routing nothing is preferable to routing with violated guarantees.

6.5 Calibration–Efficiency Separation

Figure 3 demonstrates the calibration–efficiency separation empirically. The gate’s ECE peaks at $\tau = 0$ (0.28) where class balance is near 50/50 and the gate’s probability estimates are least reliable. Yet, conformal violation remains well below $\alpha = 0.1$ at all τ . The primary cost of this initial miscalibration is threshold instability rather than strict invalidity. At $\tau = 0$, coverage is only 0.3% despite 43% of inputs being theoretically safe ($\pi = 0.43$).

As detailed in Appendix E, applying post-hoc recalibration substantially reduces ECE but does not uniformly increase coverage. Instead, by preventing the conformal procedure from selecting extreme thresholds to compensate for skewed scores, recalibration stabilizes the threshold in a denser region of the data. This occasionally results in slightly lower coverage but yields a realized violation

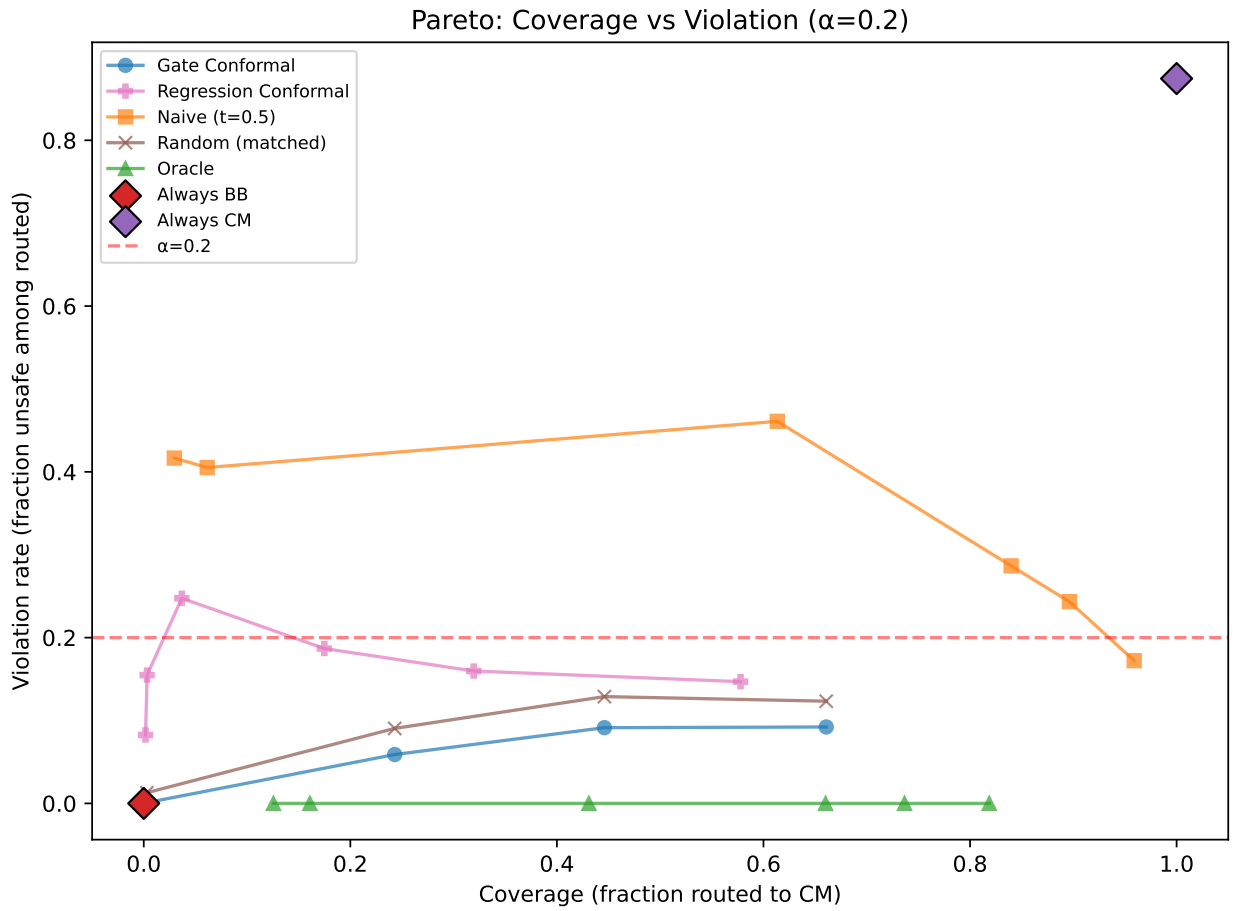


Figure 2: Coverage vs. violation rate at $\alpha = 0.2$. Each point corresponds to a τ value averaged over 35 datasets. Gate conformal remains below α . Regression conformal and naive operate above it.

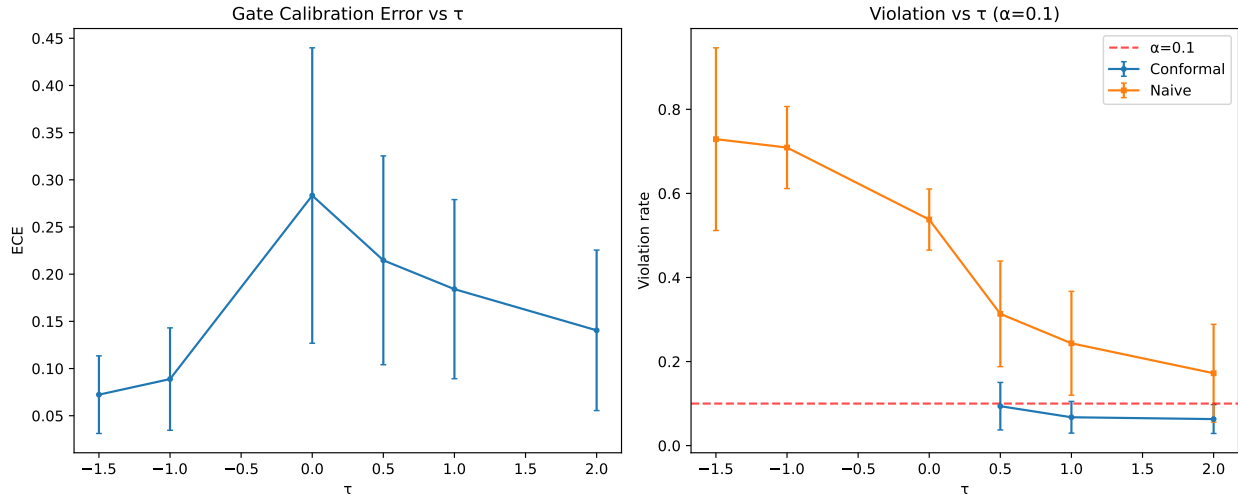


Figure 3: Left: gate ECE varies from 0.07 to 0.28 across τ . Right: despite high ECE, conformal violation remains below $\alpha = 0.1$. Naive violations are 4–8 \times higher.

rate that is more stable and truer to the underlying data distribution. Ultimately, this indicates that while proper calibration stabilizes thresholds, the remaining efficiency gap is primarily due to ranking limitations ($AUC = 0.58$), not miscalibration.

6.6 Gate Conformal vs. Regression Conformal

We next compare against the natural regression-based alternative: predict degradation $d(x)$ from input features and apply split conformal intervals, routing when the upper bound lies below τ (Section 6). This baseline has no direct guarantee on conditional violation among routed inputs, so we evaluate both coverage and violations of α per dataset.

Table 3: Per-dataset comparison at practical operating points. Gate conformal achieves higher coverage on more datasets while violating α on far fewer.

τ	α	#DS	Higher Cov.		Violates α	
			Gate	Reg	Gate	Reg
0.5	0.2	23	10	11	2	15
0.5	0.3	32	16	14	2	18
1.0	0.2	29	18	7	4	11
1.0	0.3	32	20	7	1	12
2.0	0.2	32	18	6	2	7
2.0	0.3	35	13	9	2	7

Gate conformal achieves higher coverage on more datasets while violating α far less often than regression conformal (Table 3). At $\tau = 1.0, \alpha = 0.2$, the mean coverage gain is +23.9% ($p < 0.001$, Wilcoxon signed-rank test [Demšar, 2006]).

Remark 3 (Marginal vs. conditional risk control in routing). *Split conformal regression guarantees $\Pr(d(X) \leq \hat{d}(X) + \hat{q}) \geq 1 - \alpha$ marginally over all test inputs. Routing, however, conditions on the event $\{\hat{d}(X) + \hat{q} \leq \tau\}$, which selects inputs where predicted degradation is low. This conditioning can*

concentrate the routed subset on inputs where the regression model is overconfident. The resulting conditional violation rates can far exceed α . This failure is structural, not a limitation of regressor capacity. Replacing ridge regression with a nonlinear `HistGradientBoostingRegressor` increases the violation rate from 56% to 72% of settings at $\alpha = 0.2$ (Table 10). A more accurate regressor routes more aggressively into the biased subset, making the problem worse. The classification formulation avoids this issue by directly targeting the conditional violation rate on the routed set.

6.7 Guarantee Reliability Across α

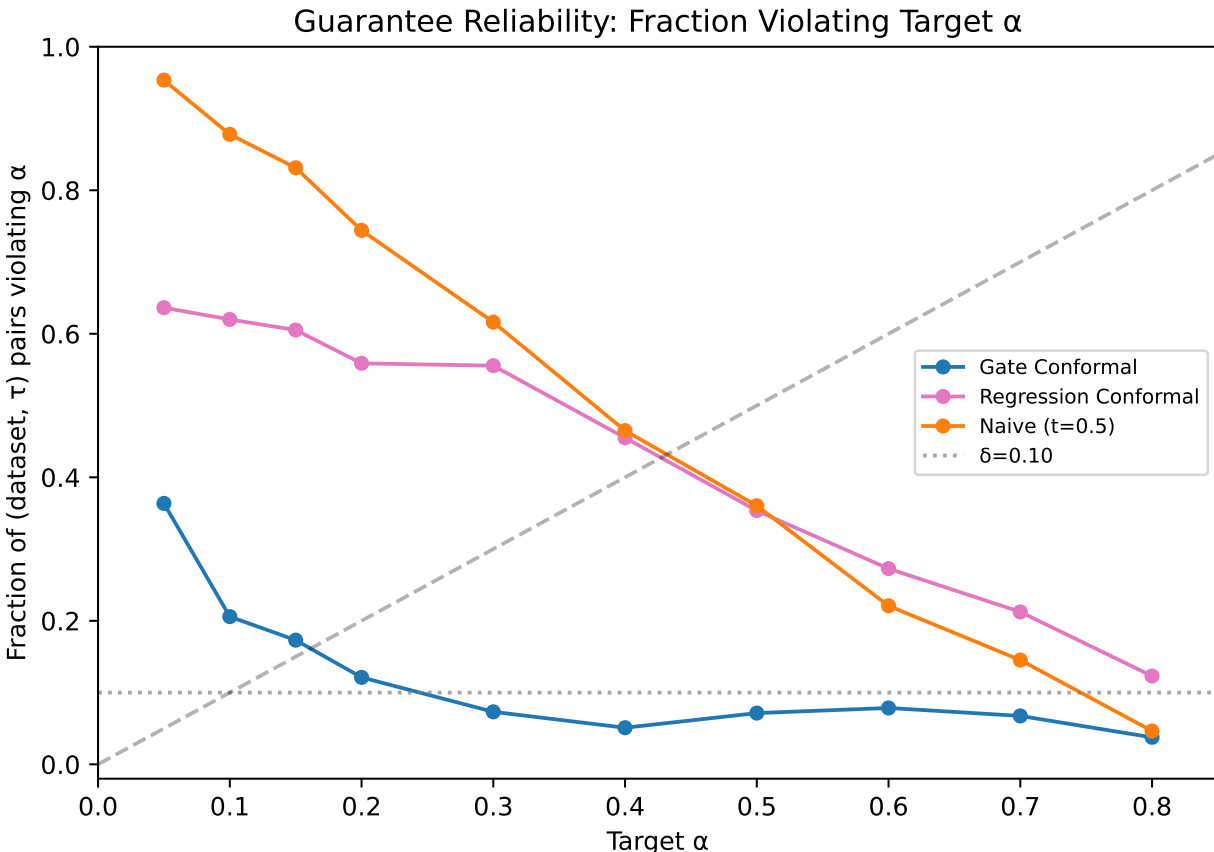


Figure 4: Fraction of $(\text{dataset}, \tau)$ pairs violating target α across the full α range. Gate conformal remains near the $\delta = 0.10$ line. Baselines converge only at very permissive α .

Figure 4 shows guarantee reliability across the full α range. Gate conformal maintains violation rates near or below $\delta = 0.10$ for $\alpha \geq 0.15$, confirming the theoretical guarantee. At very strict $\alpha = 0.05$, the rate rises to 36%. This occurs because few $(\text{dataset}, \tau)$ pairs have enough safe points in the calibration set to verify at $\alpha = 0.05$ with $\delta = 0.10$, so the denominator consists primarily of borderline cases. Regression conformal violates at 55–63% across most α values, and naive thresholding exceeds 60% at $\alpha \leq 0.3$.

We analyze calibration set size requirements in detail in Appendix D, showing that $n \approx 300$ is comfortably in the regime where the bound is tight.

7 Discussion

Practical implications. Our results suggest the following workflow for safe model routing. (1) Train a gate classifier. (2) Check feasibility via Proposition 2 using estimated π and desired α . (3) If feasible, run Algorithm 1 on a calibration set sized appropriately for the target risk level, for example ensuring $n \gg 1/\alpha$ to obtain non-vacuous bounds. (4) Deploy with formal guarantees.

Post-hoc recalibration, such as temperature scaling or beta calibration, is not required for theoretical validity but is recommended in practice. Maximum achievable coverage is primarily limited by ranking quality (AUC) rather than miscalibration. Recalibration does not substantially increase coverage, but by correcting over- or underconfident scores it prevents the conformal procedure from selecting extreme thresholds. This stabilizes finite-sample behavior and yields violation rates more closely aligned with the target α (Appendix E).

The framework requires only a gate trained on input features and a calibration set with binary safety labels. These requirements are lightweight and model-agnostic, and extend naturally to domains such as LLM routing using human evaluation or automated scoring.

Computational cost. The gate is a logistic regression requiring a single dot product per input, or $O(d)$ operations where d is the feature dimension. The expensive model is a random forest with 1500 trees, requiring $O(1500 \times \text{depth})$ operations per input. This is approximately three orders of magnitude more expensive than the gate. At 66% coverage ($\tau = 2.0$), proactive routing avoids running the expensive model on two-thirds of inputs. The gate overhead is negligible compared to either model. Unlike cascading, which must run the surrogate on every input before deciding to escalate, proactive routing runs only the gate on all inputs.

When routing fails. At $\tau = -1.0$, only 16% of inputs are safe ($\pi = 0.16$). With $\alpha = 0.2$, Proposition 2 requires

$$\frac{\text{TPR}(t)}{\text{FPR}(t)} \geq C(0.16, 0.2) = \frac{0.84 \times 0.8}{0.16 \times 0.2} = 21.$$

No empirical ROC point satisfies this, even with AUC 0.70. The sufficient bound gives $\Phi_c = 1.0$, implying that near-perfect ranking would be required.

Accordingly, conformal returns $t^* = \infty$ and abstains. Regression conformal instead routes 0.3% of inputs with 15.5% mean violation, exceeding α on most datasets.

Classification vs. regression for routing. The dominance of classification over regression in our setting has a clear explanation: predicting whether $d(x) \leq \tau$ (a binary question) requires only finding a decision boundary, while predicting $d(x)$ (a continuous quantity) requires accurate function approximation everywhere. When input features are weakly predictive of degradation (as in our tabular setting), the classification formulation degrades gracefully (lower coverage) while the regression formulation leads to frequent violations.

Limitations. Several limitations bound our conclusions and suggest directions for future work.

Marginal vs. conditional guarantees. Our guarantee controls the average violation rate over random draws of the calibration set, not the violation rate conditional on specific input subregions. Exact distribution-free conditional coverage is known to be impossible without structural assumptions [Angelopoulos and Bates, 2022]. The routed set could therefore contain subgroups with higher-than- α violation rates even while the overall rate is controlled. Extending to approximate conditional guarantees via group-conditional conformal methods is an important direction.

Tolerance selection. We report results across multiple degradation tolerances τ for analysis, running the conformal procedure independently for each (τ, α) pair. In deployment, τ represents an application-dependent tolerance. If a practitioner wishes to select τ adaptively using calibration data, a separate tuning split or a Learn-Then-Test style procedure [Angelopoulos et al., 2022] can be used to preserve the nominal δ guarantee.

Exchangeability and distribution shift. The guarantee assumes calibration and test data are exchangeable. Under covariate shift, where $P_{\text{test}}(X) \neq P_{\text{cal}}(X)$, the guarantee formally breaks. The Clopper–Pearson bound is exact (finite-sample), so mild distribution shift may not immediately produce empirical violations, but the formal guarantee no longer applies. Weighted conformal prediction [Tibshirani et al., 2020], which reweights calibration points by likelihood ratios $dP_{\text{test}}/dP_{\text{cal}}$, could extend the framework to known shift. However, estimating these ratios introduces additional uncertainty.

Empirically, we observe that even under assumed exchangeability, finite-sample variability across different random splits can lead to realized violation rates slightly exceeding δ for strict α targets.

Input-space separability. Coverage is fundamentally bounded by how well input features x separate safe from unsafe regions. If degradation depends primarily on label noise or model stochasticity rather than input features, no gate can achieve high AUC, and coverage will be low regardless of calibration or conformal procedure. This is a limitation of the routing problem itself, not our method: some model pairs on some data simply do not admit efficient input-based routing.

8 Conclusion

We introduced proactive routing to interpretable surrogates with exact, distribution-free safety guarantees. A classification gate predicts input-level safety, and Clopper–Pearson conformal calibration selects a routing threshold that controls the violation rate on the routed subset with probability $1 - \delta$. Our analysis characterizes routing feasibility through a likelihood-ratio condition and a sufficient critical AUC bound, clarifying when safe routing is achievable. Across 35 datasets and multiple model families, gate conformal routing achieves higher coverage with controlled violations compared to regression-based baselines. Future work includes extensions to hierarchical routing frameworks and robustness under distribution shift.

References

- Anastasios N. Angelopoulos and Stephen Bates. A gentle introduction to conformal prediction and distribution-free uncertainty quantification, 2022. URL <https://arxiv.org/abs/2107.07511>.
- Anastasios N. Angelopoulos, Stephen Bates, Emmanuel J. Candès, Michael I. Jordan, and Lihua Lei. Learn then test: Calibrating predictive algorithms to achieve risk control, 2022. URL <https://arxiv.org/abs/2110.01052>.
- Stephen Bates, Anastasios Angelopoulos, Lihua Lei, Jitendra Malik, and Michael I. Jordan. Distribution-free, risk-controlling prediction sets. *Journal of the ACM*, 68(6), 2021. doi: 10.1145/3478535.
- Leo Breiman. Random forests. *Machine Learning*, 45(1):5–32, 2001. doi: 10.1023/A:1010933404324.
- Tianqi Chen and Carlos Guestrin. Xgboost: A scalable tree boosting system. In *Proceedings of the 22nd ACM SIGKDD International Conference on Knowledge Discovery and Data Mining*, pages 785–794, 2016. doi: 10.1145/2939672.2939785.

- Lingjiao Chen, Matei Zaharia, and James Zou. Frugalgpt: How to use large language models while reducing cost and improving performance, 2023. URL <https://arxiv.org/abs/2305.05176>.
- C. K. Chow. On optimum recognition error and reject tradeoff. *IEEE Transactions on Information Theory*, 16(1):41–46, 1970. doi: 10.1109/TIT.1970.1054406.
- C. J. Clopper and E. S. Pearson. The use of confidence or fiducial limits illustrated in the case of the binomial. *Biometrika*, 26(4):404–413, 1934. doi: 10.1093/biomet/26.4.404.
- Janez Demšar. Statistical comparisons of classifiers over multiple data sets. *Journal of Machine Learning Research*, 7:1–30, 2006.
- Dujian Ding, Ankur Mallick, Chi Wang, Robert Sim, Subhabrata Mukherjee, Victor Ruhle, Laks V. S. Lakshmanan, and Ahmed Hassan Awadallah. Hybrid LLM: Cost-efficient and quality-aware query routing. *arXiv preprint arXiv:2404.14618*, 2024. URL <https://arxiv.org/abs/2404.14618>.
- Ran El-Yaniv and Yair Wiener. On the foundations of noise-free selective classification. *Journal of Machine Learning Research*, 11:1605–1641, 2010.
- Tom Fawcett. An introduction to roc analysis. *Pattern Recognition Letters*, 27(8):861–874, 2006. doi: 10.1016/j.patrec.2005.10.010.
- Yonatan Geifman and Ran El-Yaniv. Selective classification for deep neural networks. In *Advances in Neural Information Processing Systems*, volume 30, 2017.
- Ian Goodfellow, Yoshua Bengio, and Aaron Courville. *Deep Learning*. MIT Press, 2016. <http://www.deeplearningbook.org>.
- Chuan Guo, Geoff Pleiss, Yu Sun, and Kilian Q. Weinberger. On calibration of modern neural networks. In *Proceedings of the 34th International Conference on Machine Learning*, pages 1321–1330, 2017.
- Geoffrey Hinton, Oriol Vinyals, and Jeff Dean. Distilling the knowledge in a neural network. *arXiv preprint arXiv:1503.02531*, 2015. URL <https://arxiv.org/abs/1503.02531>.
- Arthur E Hoerl and Robert W Kennard. Ridge regression: Biased estimation for nonorthogonal problems. *Technometrics*, 12(1):55–67, 1970.
- Robert A Jacobs, Michael I Jordan, Steven J Nowlan, and Geoffrey E Hinton. Adaptive mixtures of local experts. *Neural Computation*, 3(1):79–87, 1991.
- Meelis Kull, Telmo Silva Filho, and Peter Flach. Beta calibration: a well-founded and easily implemented improvement on logistic calibration for binary classifiers. In *Proceedings of the 20th International Conference on Artificial Intelligence and Statistics*, pages 623–631, 2017.
- Jing Lei, Max G’Sell, Alessandro Rinaldo, Ryan J Tibshirani, and Larry Wasserman. Distribution-free predictive inference for regression. *Journal of the American Statistical Association*, 113(523): 1094–1111, 2018.
- Scott M Lundberg and Su-In Lee. A unified approach to interpreting model predictions. In *Advances in Neural Information Processing Systems*, volume 30, 2017.

- David Madras, Toniann Pitassi, and Richard Zemel. Predict responsibly: Improving fairness and accuracy by learning to defer. In *Advances in Neural Information Processing Systems*, volume 31, 2018.
- Ruth Marcus, Eric Peritz, and K. R. Gabriel. On closed testing procedures with special reference to ordered analysis of variance. *Biometrika*, 63(3):655–660, 1976. doi: 10.1093/biomet/63.3.655.
- Jerzy Neyman and Egon S. Pearson. On the problem of the most efficient tests of statistical hypotheses. *Philosophical Transactions of the Royal Society of London. Series A*, 231:289–337, 1933. doi: 10.1098/rsta.1933.0009.
- Alexandru Niculescu-Mizil and Rich Caruana. Predicting good probabilities with supervised learning. In *Proceedings of the 22nd International Conference on Machine Learning*, pages 625–632, 2005.
- William Overman and Mohsen Bayati. Conformal arbitrage: Risk-controlled balancing of competing objectives in language models. In *Advances in Neural Information Processing Systems (NeurIPS)*, 2025. URL <https://arxiv.org/abs/2506.00911>.
- Harris Papadopoulos, Kostas Proedrou, Volodya Vovk, and Alex Gammerman. Inductive confidence machines for regression. In *European Conference on Machine Learning*, pages 345–356. Springer, 2002.
- John Platt. Probabilistic outputs for support vector machines and comparisons to regularized likelihood methods. In *Advances in Large Margin Classifiers*, pages 61–74, 1999.
- Marco Tulio Ribeiro, Sameer Singh, and Carlos Guestrin. “Why should i trust you?”: Explaining the predictions of any classifier. In *Proceedings of the 22nd ACM SIGKDD International Conference on Knowledge Discovery and Data Mining*, pages 1135–1144, 2016. doi: 10.1145/2939672.2939778.
- Yaniv Romano, Evan Patterson, and Emmanuel Candès. Conformalized quantile regression. In *Advances in Neural Information Processing Systems*, volume 32, 2019.
- Cynthia Rudin. Stop explaining black box machine learning models for high stakes decisions and use interpretable models instead. *Nature Machine Intelligence*, 1(5):206–215, 2019. doi: 10.1038/s42256-019-0048-x.
- Ryan J. Tibshirani, Rina Foygel Barber, Emmanuel J. Candès, and Aaditya Ramdas. Conformal prediction under covariate shift. *arXiv preprint arXiv:1904.06019*, 2020. URL <https://arxiv.org/abs/1904.06019>.
- Kirill Trapeznikov and Venkatesh Saligrama. Supervised sequential classification under budget constraints. In *Proceedings of the 16th International Conference on Artificial Intelligence and Statistics*, pages 581–589, 2013.
- Antonios Valkanas, Soumyasundar Pal, Pavel Rumiantsev, Yingxue Zhang, and Mark Coates. C3po: Optimized large language model cascades with probabilistic cost constraints for reasoning. *arXiv preprint arXiv:2511.07396*, 2025. URL <https://arxiv.org/abs/2511.07396>.
- Joaquin Vanschoren, Jan N. van Rijn, Bernd Bischl, and Luis Torgo. OpenML: Networked science in machine learning. *SIGKDD Explorations*, 15(2):49–60, 2014. doi: 10.1145/2641190.2641198.
- Paul Viola and Michael Jones. Rapid object detection using a boosted cascade of simple features. In *Proceedings of the IEEE Conference on Computer Vision and Pattern Recognition (CVPR)*, volume 1, pages 511–518, 2001. doi: 10.1109/CVPR.2001.990517.

- Vladimir Vovk, Alex Gammerman, and Glenn Shafer. *Algorithmic Learning in a Random World*. Springer, 2005. doi: 10.1007/b106715.
- Xin Wang, Fisher Yu, Zi-Yi Dou, Trevor Darrell, and Joseph E. Gonzalez. Skipnet: Learning dynamic routing in convolutional networks. In *Proceedings of the European Conference on Computer Vision (ECCV)*, pages 409–424, 2018.
- Zhiyuan Wang, Aniri, Tianlong Chen, Yue Zhang, Heng Tao Shen, Xiaoshuang Shi, and Kaidi Xu. A linear expectation constraint for selective prediction and routing with false-discovery control. *arXiv preprint arXiv:2512.01556*, 2026. URL <https://arxiv.org/abs/2512.01556>.
- Zuxuan Wu, Tushar Nagarajan, Abhishek Kumar, Steven Rennie, Larry S. Davis, Kristen Grauman, and Rogerio Feris. Blockdrop: Dynamic inference paths in residual networks. In *Proceedings of the IEEE Conference on Computer Vision and Pattern Recognition (CVPR)*, pages 8817–8826, 2018.
- Bianca Zadrozny and Charles Elkan. Transforming classifier scores into accurate multiclass probability estimates. In *Proceedings of the Eighth ACM SIGKDD International Conference on Knowledge Discovery and Data Mining*, pages 694–699, 2002. doi: 10.1145/775047.775151.
- Lucas Zimmer, Marius Lindauer, and Frank Hutter. Auto-PyTorch: Multi-fidelity metalearning for efficient and robust AutoDL. *IEEE Transactions on Pattern Analysis and Machine Intelligence*, 43(9):3079–3090, 2021. doi: 10.1109/TPAMI.2021.3067763.

A Proofs

A.1 Proof of Proposition 1

The guarantee follows from the coverage property of Clopper–Pearson intervals combined with the fixed-sequence testing argument of Remark 1. For any fixed threshold t , let $p^* = V(t)$ denote the true violation rate. On the calibration set, $k(t) \sim \text{Binomial}(n(t), p^*)$. By the Clopper–Pearson construction [Clopper and Pearson, 1934]:

$$\Pr(p^* \leq \text{UCB}_\delta(k(t), n(t))) \geq 1 - \delta.$$

Algorithm 1 selects t^* adaptively from $\{t_1, \dots, t_m\}$. Conditioning on the gate scores $\{s_i\}_{i=1}^n$, the threshold ordering and routed index sets become deterministic. The labels $\{Y_i\}$ remain exchangeable conditional on the scores because the gate is trained on an independent split. Each conditional CP test is therefore exact. The fixed-sequence testing principle [Marcus et al., 1976] ensures that accepting the first threshold satisfying $\text{UCB}_\delta \leq \alpha$ in a pre-specified order controls the family-wise error rate at level δ . By iterated expectation, $\Pr(V(t^*) > \alpha) \leq \delta$ holds unconditionally.

This argument requires that the calibration set is independent of the gate training data and that calibration points are exchangeable with test points. Our 4-way split ensures both conditions. The Clopper–Pearson bound is exact and not asymptotic, so the guarantee holds for any sample size n .

A.2 Proof of Theorem 1

The ROC curve $\{(\text{FPR}(t), \text{TPR}(t)) : t \in \mathbb{R}\}$ satisfies $\text{AUC} = \int_0^1 \text{TPR}(u) du$ where $u = \text{FPR}$.

Suppose no point on the ROC satisfies (6), i.e., $\text{TPR}(u) < C(\pi, \alpha) \cdot u$ for all $u \in (0, 1]$. Then:

$$\text{AUC} = \int_0^1 \text{TPR}(u) du < \int_0^1 C \cdot u du = \frac{C}{2}.$$

Taking the contrapositive: if $\text{AUC} \geq C/2 = \Phi_c(\pi, \alpha)$, then there exists a point satisfying (6). Since $\text{AUC} \leq 1$, we clip at 1.

Note this is a necessary condition for infeasibility, not sufficient for feasibility: $\text{AUC} \geq \Phi_c$ guarantees some point on the ROC has high enough likelihood ratio, but a non-concave ROC could still have that point at a degenerate threshold.

A.3 Proof of Proposition 2

Proof. By Bayes’ rule: $V(t) = \frac{(1-\pi)\text{FPR}(t)}{(1-\pi)\text{FPR}(t) + \pi\text{TPR}(t)}$. Setting $V(t) \leq \alpha$: $(1-\pi)\text{FPR}(t) \leq \alpha[(1-\pi)\text{FPR}(t) + \pi\text{TPR}(t)]$, which rearranges to $(1-\alpha)(1-\pi)\text{FPR}(t) \leq \alpha\pi\text{TPR}(t)$. Dividing both sides by $\text{FPR}(t)$ (assumed positive for non-trivial routing) gives (6). \square

B Regression Conformal Baseline Details

The regression conformal baseline trains Ridge regression ($\alpha_{\text{Ridge}} = 1.0$) to predict $d(x)$ from input features. On the calibration set, it computes residuals $r_i = d_i - \hat{d}_i$. For each target α , it finds the conformal quantile:

$$\hat{q} = \text{Quantile}\left(r_1, \dots, r_n; \frac{\lceil (n+1)(1-\alpha) \rceil}{n}\right),$$

and routes input x to the surrogate iff $\hat{d}(x) + \hat{q} \leq \tau$.

This is a standard split conformal prediction interval [Romano et al., 2019] applied to the degradation prediction problem. It guarantees $\Pr(d(X) \leq \hat{d}(X) + \hat{q}) \geq 1 - \alpha$ marginally, but the routing decision $\hat{d}(x) + \hat{q} \leq \tau$ provides no direct guarantee on the violation rate among routed inputs. This is because the conformal guarantee is marginal over all test points, not conditional on the routed subset.

B.1 Proof of Theorem 2

Lemma 1 (Concave secant property). *For a concave function $f : [0, 1] \rightarrow [0, 1]$ with $f(0) = 0$, the secant $f(u)/u$ is non-increasing on $(0, 1]$.*

Proof. For $0 < a < b \leq 1$, concavity gives $f(a) \geq \frac{a}{b}f(b) + (1 - \frac{a}{b})f(0) = \frac{a}{b}f(b)$, so $f(a)/a \geq f(b)/b$. \square

Proof of Theorem 2. Case $C \leq 1$: At $u = 1$: $\text{ROC}(1)/1 = 1 \geq C$. Feasibility holds trivially (routing all inputs satisfies $V \leq \alpha$).

Case $C > 1$:

(i) *Sufficiency.* By Lemma 1, $\sup_{u \in (0, 1]} \text{ROC}(u)/u = \text{ROC}'(0^+) \triangleq L$. Infeasibility means $L < C$. For a concave ROC with initial slope L , the curve lies below $\min(Lu, 1)$, so

$$\text{AUC} \leq \int_0^{1/L} Lu \, du + \int_{1/L}^1 1 \, du = \frac{1}{2L} + 1 - \frac{1}{L} = 1 - \frac{1}{2L}.$$

Since $L < C$: $\text{AUC} < 1 - 1/(2C) = \Phi_c^*$. Contrapositive: $\text{AUC} \geq \Phi_c^*$ implies feasibility.

(ii) *Tightness.* For any $\varepsilon > 0$, choose $L = C - \eta$ with $\eta > 0$ small enough that $1 - 1/(2L) > \Phi_c^* - \varepsilon$. The concave ROC $\text{ROC}(u) = \min(Lu, 1)$ has $\text{ROC}'(0^+) = L < C$ (infeasible) and $\text{AUC} = 1 - 1/(2L) \rightarrow \Phi_c^*$ as $\eta \rightarrow 0$.

(iii) *Comparison.* For $C > 1$: $\Phi_c^* = 1 - \frac{1}{2C} < \frac{C}{2} = \Phi_c$ iff $2C - 1 < C^2$ iff $(C - 1)^2 > 0$, which holds for all $C \neq 1$. \square

B.2 Proof of Theorem 3

Proof. Let $\text{ROC} : [0, 1] \rightarrow [0, 1]$ denote the (achievable) concave ROC curve of the gate, where $u = \text{FPR}$ and $v = \text{TPR}$, and suppose $\text{AUC} = A \geq \Phi_c^*$. Let $C = C(\pi, \alpha) > 1$. By Proposition 2, feasibility requires an operating point (u, v) with $v/u \geq C$. For any threshold achieving $v = Cu$, the routed coverage is

$$\text{Cov}(u) = (1 - \pi)u + \pi v = ((1 - \pi) + \pi C)u.$$

Using $C = (1 - \pi)(1 - \alpha)/(\pi\alpha)$, we have

$$(1 - \pi) + \pi C = (1 - \pi) + \frac{(1 - \pi)(1 - \alpha)}{\alpha} = \frac{1 - \pi}{\alpha},$$

so $\text{Cov}(u) = \frac{1 - \pi}{\alpha} u$ on the feasibility boundary $v = Cu$.

Define

$$u_{\max} := \sup\{u \in [0, 1] : \text{ROC}(u) \geq Cu\}.$$

Concavity implies that the secant $\text{ROC}(u)/u$ is non-increasing in u , hence the feasible set is an interval $[0, u_{\max}]$ and $\text{ROC}(u_{\max}) = Cu_{\max}$ (when $u_{\max} < 1$). It suffices to lower bound u_{\max} in terms of A and C .

Consider the piecewise-linear ROC that is linear from $(0, 0)$ to (u_{\max}, Cu_{\max}) and then linear from (u_{\max}, Cu_{\max}) to $(1, 1)$. This curve is concave and, among concave ROC curves with the same u_{\max} and boundary point (u_{\max}, Cu_{\max}) , it minimizes area (placing as much mass as possible on the chord). Therefore, any concave ROC with the same u_{\max} has AUC at least that of this two-segment curve.

A direct geometric calculation for the two-segment curve gives

$$\text{AUC} = \frac{1 + (C - 1)u_{\max}}{2}.$$

Thus, if $\text{AUC} = A$, then necessarily

$$A \geq \frac{1 + (C - 1)u_{\max}}{2} \implies u_{\max} \geq \frac{2A - 1}{C - 1}.$$

Since $u_{\max} \leq 1$, we obtain

$$u_{\max} \geq \min\left\{1, \frac{2A - 1}{C - 1}\right\}.$$

Finally, choosing the threshold at $u = u_{\max}$ on the boundary yields

$$\begin{aligned} \text{Cov}^* &\geq \frac{1 - \pi}{\alpha} u_{\max} \\ &\geq \min\left\{1, \frac{(2A - 1)(1 - \pi)}{(C - 1)\alpha}\right\}. \end{aligned}$$

which proves the claim.

Tightness. Equality is achieved by the two-segment concave ROC constructed above, with breakpoint (u_{\max}, Cu_{\max}) and $u_{\max} = \min\{1, (2A - 1)/(C - 1)\}$. \square

C Full Results

Table 4: Gate conformal vs. regression conformal: mean coverage and violation across 35 datasets at representative operating points.

τ	α	Gate Cov.	Gate Viol.	Reg Cov.	Reg Viol.
0.5	0.10	0.096	0.021	0.073	0.098
0.5	0.20	0.243	0.059	0.175	0.187
0.5	0.30	0.431	0.134	0.335	0.320
1.0	0.10	0.132	0.015	0.122	0.064
1.0	0.20	0.446	0.091	0.320	0.160
1.0	0.30	0.638	0.145	0.550	0.253
2.0	0.10	0.351	0.032	0.269	0.079
2.0	0.20	0.661	0.092	0.578	0.147
2.0	0.30	0.847	0.134	0.754	0.175

Table 5: Significance tests (Wilcoxon signed-rank, two-sided). To evaluate operational tradeoffs, tests are conditioned on problem instances where both methods successfully found a valid routing threshold (coverage ≥ 0). Under these conditions, Gate Conformal achieves significantly lower violation rates than the naive baseline and significantly higher coverage than regression conformal.

Comparison	τ, α	Diff.	p -value	n
<i>Gate vs. Naive (violation rate):</i>				
	0.5, 0.2	-0.076	0.007	14
	1.0, 0.2	-0.060	0.002	23
	2.0, 0.2	-0.025	0.009	28
<i>Gate vs. Reg. Conformal (coverage):</i>				
	0.5, 0.2	+0.256	0.005	13
	1.0, 0.2	+0.239	<0.001	20
	2.0, 0.2	+0.139	<0.001	26

D Additional Model Pair: XGBoost vs. Decision Tree

To verify that our conclusions are not specific to the random forest / decision tree pairing used in the main text, we repeated the full evaluation using an XGBoost model as the expensive predictor and a decision tree as the surrogate on the same 35 OpenML regression datasets. All experimental settings (data splits, calibration size, risk levels α , and tolerance levels τ) were kept identical.

D.0 Model Details (XGBoost)

For the additional robustness experiment, the expensive model f was implemented as an XGBoost regressor with the following hyperparameters:

- `n_estimators = 1500`
- `learning_rate = 0.03`
- `max_depth = 6`
- `subsample = 0.9`
- `colsample_bytree = 0.9`
- `reg_lambda = 1.0`
- `random_state = fixed`
- `n_jobs = -1`

All other experimental settings (splits, calibration procedure, surrogate depth selection, and risk levels) were identical to the main experiment.

D.1 Gate Properties

Table 6 reports gate statistics across tolerance levels.

Table 6: Gate properties for XGBoost vs. Decision Tree across τ . AUC is reported as median across datasets.

τ	π	AUC (median)	ECE
-1.5	0.135	0.50	0.137
-1.0	0.173	0.50	0.170
0.0	0.459	0.51	0.302
0.5	0.639	0.58	0.213
1.0	0.717	0.56	0.160
2.0	0.799	0.57	0.136

The same structural patterns observed in the main paper persist: (i) feasibility is primarily driven by the base safe rate π , and (ii) moderate AUC values (≈ 0.55 – 0.60) suffice when π is large.

D.2 Guarantee Reliability

We evaluate the fraction of (dataset, τ) pairs violating the target α . Results are consistent with the finite-sample guarantee:

- At $\alpha = 0.10$: 14.3% violation rate.
- At $\alpha = 0.20$: 12.1% violation rate.
- At $\alpha = 0.30$: 14.5% violation rate.
- At $\alpha = 0.50$: 5.1% violation rate.

For $\alpha \geq 0.20$, violation rates remain close to the target confidence level $\delta = 0.10$, matching the behavior observed in the random forest setting.

Regression conformal violates α at substantially higher rates (31%–37% for $\alpha \in \{0.10, 0.20, 0.30\}$), confirming that the superiority of the classification-based gate formulation is not model-pair specific.

D.3 Coverage–Violation Tradeoffs

Across practical operating points ($\tau \geq 0.5$), gate conformal consistently achieves higher coverage than regression conformal while maintaining comparable or lower violation rates.

For example:

- $\tau = 1.0$, $\alpha = 0.2$: Gate coverage = 0.419 vs. 0.310 (regression), with similar violation rates.
- $\tau = 2.0$, $\alpha = 0.2$: Gate coverage = 0.619 vs. 0.543.

Per-dataset comparisons show that gate conformal achieves higher coverage on a majority of datasets at $\tau \in \{1.0, 2.0\}$ and $\alpha \in \{0.2, 0.3\}$.

Wilcoxon signed-rank tests confirm statistically significant coverage improvements at multiple operating points (e.g., $\tau = 1.0$, $\alpha = 0.2$, $p = 0.0033$).

D.4 Summary

The XGBoost results are consistent with the main findings:

1. The conformal guarantee holds across α .
2. Feasibility depends primarily on π , not absolute AUC.
3. Classification-based routing dominates regression conformal in coverage.
4. When routing is infeasible, the method abstains rather than violating safety.

These results demonstrate that the proposed framework is model-agnostic and not tied to a specific black-box architecture.

E Additional Model Pair: MLP vs. Decision Tree

To further assess robustness across model families, we repeated all experiments using a multilayer perceptron (MLP) as the expensive model and a decision tree as the surrogate on the same 35 OpenML regression datasets.

E.1 Model Details

The expensive model f was implemented using a multilayer perceptron with the following architecture:

- Hidden layers: (256, 128, 64)
- Activation: ReLU
- Optimizer: Adam
- Weight decay: $\alpha = 10^{-4}$
- Learning rate: 10^{-3}
- Max iterations: 1000
- Early stopping enabled (validation fraction 0.1)
- Random seed fixed

All preprocessing, data splits, calibration size, risk levels α , and tolerance values τ were identical to the main experiment.

E.2 Gate Properties

Table 7 summarizes gate statistics across tolerance levels.

Table 7: Gate properties for MLP vs. Decision Tree.

τ	π	AUC (median)	ECE
-1.5	0.300	0.688	0.122
-1.0	0.368	0.627	0.154
0.0	0.629	0.544	0.221
0.5	0.723	0.570	0.194
1.0	0.770	0.557	0.153
2.0	0.830	0.535	0.112

As in the main paper, feasibility is primarily governed by the safe base rate π . Even moderate AUC values (≈ 0.55 – 0.60) suffice when π is large, consistent with Proposition 2 and Theorem 1.

E.3 Guarantee Reliability

The conformal guarantee remains well-calibrated across risk levels:

- $\alpha = 0.10$: 10.3% violation rate.
- $\alpha = 0.20$: 16.5% violation rate.
- $\alpha = 0.30$: 13.6% violation rate.
- $\alpha = 0.50$: 5.5% violation rate.

These rates remain close to the nominal confidence parameter $\delta = 0.10$ for $\alpha \geq 0.20$, mirroring behavior observed with RF and XGBoost.

In contrast, regression conformal violates α at substantially higher rates (50%–71% for $\alpha \in \{0.10, 0.20, 0.30\}$).

E.4 Coverage–Violation Tradeoffs

Across practical operating points ($\tau \geq 0.5$), gate conformal achieves substantially higher coverage than regression conformal while maintaining lower or comparable violation rates.

For example:

- $\tau = 1.0, \alpha = 0.2$: Gate coverage = 0.471 vs. 0.342 (regression), with lower violation.
- $\tau = 2.0, \alpha = 0.2$: Gate coverage = 0.700 vs. 0.532.

Per-dataset comparisons show that gate conformal wins on a majority of datasets at all practical operating points. For instance:

- $\tau = 1.0, \alpha = 0.2$: Gate wins 18 vs. 7 datasets on coverage.
- $\tau = 2.0, \alpha = 0.2$: Gate wins 22 vs. 4 datasets.

Wilcoxon signed-rank tests confirm statistically significant coverage improvements across nearly all practical regimes (e.g., $\tau = 1.0, \alpha = 0.2, p = 5 \times 10^{-4}$).

E.5 Summary

The MLP results replicate and strengthen all main findings:

1. The conformal guarantee remains reliable.
2. Feasibility depends primarily on π rather than absolute AUC.
3. Classification-based routing substantially outperforms regression conformal in coverage.
4. When routing is infeasible, the method abstains rather than violating safety.

These experiments indicate that the framework is robust across tree-based, boosting-based, and neural network black-box models.

D Calibration Set Size Requirements

The Clopper–Pearson bound tightens rapidly with calibration set size. Table 8 shows the upper confidence bound $UCB_{0.10}(k, n)$ for representative (k, n) combinations. With $n = 300$ (our setup: 15% of 2000 configurations), observing $k = 0$ unsafe among routed calibration points yields $UCB = 0.008$. Even with $k = 10$ unsafe out of $n = 100$ routed points, $UCB = 0.150$, which remains below $\alpha = 0.2$.

Table 8: Clopper–Pearson upper bounds $UCB_{0.10}(k, n)$ for selected calibration set sizes. With $n \approx 300$, the bound is sufficiently tight for practical risk control.

k unsafe	Calibration points routed (n)				
	50	100	200	300	500
0	0.045	0.023	0.011	0.008	0.005
1	0.076	0.038	0.019	0.013	0.008
5	0.178	0.091	0.046	0.031	0.018
10	0.291	0.150	0.076	0.051	0.031
20	—	0.261	0.133	0.089	0.054

The minimum calibration size required to guarantee $V(t^*) \leq \alpha$ when the true violation rate is zero satisfies $n \geq \lceil \log(\delta) / \log(1 - \alpha) \rceil$. For $\alpha = 0.2$, $\delta = 0.1$: $n \geq 11$; for $\alpha = 0.05$, $\delta = 0.1$: $n \geq 45$. In practice, larger n is needed because some routed calibration points will be unsafe ($k > 0$), but these bounds show that even modest calibration sets provide meaningful guarantees. Our $n \approx 300$ is comfortably in the regime where the bound is tight.

E Effect of Post-Hoc Recalibration

To test whether improving gate calibration recovers coverage lost to miscalibration, we applied three post-hoc recalibration methods to the Platt-scaled gate scores: beta calibration [Kull et al., 2017], temperature scaling (logistic recalibration) [Guo et al., 2017], and isotonic regression. Each recalibrator was fit on a held-out validation set and then applied to calibration and test scores prior to conformal threshold selection. Because recalibration was learned independently of the calibration set, the exchangeability between calibration and test data required for the conformal guarantee is preserved.

Table 9: Effect of post-hoc recalibration at $\alpha = 0.2$, averaged over 35 datasets (RF vs. decision tree). Recalibration substantially reduces ECE but does not increase coverage, indicating the efficiency gap is dominated by ranking limitations.

τ	Recalibration	ECE	Coverage	Violation
0.5	None (Platt)	0.215	0.243	0.059
0.5	Beta	0.066	0.243	0.059
0.5	Temperature	0.077	0.243	0.059
0.5	Isotonic	0.050	0.216	0.043
1.0	None (Platt)	0.184	0.446	0.091
1.0	Beta	0.060	0.421	0.085
1.0	Temperature	0.071	0.421	0.085
1.0	Isotonic	0.048	0.398	0.072
2.0	None (Platt)	0.141	0.661	0.092
2.0	Beta	0.052	0.651	0.095
2.0	Temperature	0.061	0.644	0.091
2.0	Isotonic	0.036	0.622	0.077

Table 9 shows that beta calibration reduces ECE by $3\times$ (e.g., 0.184 to 0.060 at $\tau = 1.0$) while coverage decreases only slightly (-2.5pp for beta/temperature, -4.8pp for isotonic). Violation rates also decrease marginally, and the conformal guarantee continues to hold: the fraction of (dataset, τ) pairs violating α remains near $\delta = 0.10$ for all recalibration methods.

The small coverage decrease (rather than increase) indicates that the Platt-scaled gate was mildly overconfident on borderline-unsafe inputs. Recalibration corrects these scores downward, removing a small number of inputs that should not have been routed. The dominant source of the efficiency gap between our gate (42–45% coverage at $\tau = 1.0$) and the oracle (74%) is ranking quality (AUC = 0.58), not miscalibration. Improving coverage substantially would require a stronger gate, not better calibration.

E.1 Stronger Regression Baseline

To assess whether regression-conformal underperforms due to limited model capacity, we replaced ridge regression with `HistGradientBoostingRegressor` (HGBR) while keeping the conformal procedure unchanged. Results were qualitatively similar, with no improvement in violation control or coverage. This suggests that the observed gap reflects the formulation (binary risk control vs. magnitude regression) rather than regressor expressiveness.

Table 10 reports the empirical frequency of exceeding the target α across (dataset, τ) pairs. As expected, gate conformal remains broadly consistent with the nominal $\delta = 0.10$ bound, while baselines substantially exceed the target rate. Note that the conformal guarantee bounds the probability (over calibration randomness) that the routed-set violation exceeds α ; aggregation across (dataset, τ) pairs may therefore exceed α in a fraction of cases bounded by δ .

Table 10: Guarantee check across (dataset, τ) pairs when regression-conformal uses `HistGradientBoostingRegressor`. For each target α , we report the fraction of pairs whose realized violation rate exceeds α , along with mean violation rate and mean coverage.

α	Method	Violations	Mean Viol.	Mean Cov.
0.10	Gate Conf.	7/34 (21%)	0.071	0.595
	HGBR Conf.	93/119 (78%)	0.385	0.164
	Naive 0.5	151/172 (88%)	0.404	0.692
0.20	Gate Conf.	8/66 (12%)	0.129	0.717
	HGBR Conf.	128/177 (72%)	0.406	0.249
	Naive 0.5	128/172 (74%)	0.404	0.692
0.30	Gate Conf.	6/82 (7%)	0.181	0.826
	HGBR Conf.	132/196 (67%)	0.426	0.351
	Naive 0.5	106/172 (62%)	0.404	0.692
0.50	Gate Conf.	8/112 (7%)	0.278	0.917
	HGBR Conf.	90/202 (45%)	0.424	0.547
	Naive 0.5	62/172 (36%)	0.404	0.692

F GENERAL-PURPOSE OPENML REGRESSION DATASETS

To verify that our conclusions extend beyond hyperparameter configuration data, we replicate the evaluation on 22 general-purpose OpenML regression datasets spanning diverse domains: air quality (no2, pm10), social/labor (strikes), energy efficiency, medical (tumor), chemistry/biology (QSAR_Bioconcentration, physiochemical_protein), aerospace (Ailerons, NASA_PHM2008), control systems (pol), business (Job_Profitability), real estate (miami_housing, california_houses, house_sales, house_16H), transport (Bike_Sharing_Demand), physics (superconduct), energy IoT (appliances_energy_prediction), robotics (sarcos), media (Online-NewsPopularity), and classic benchmarks (2dplanes, fried). Dataset sizes range from 500 to 45,000 rows with 7 to 82 features.

Unlike the LCBench experiments where inputs are hyperparameter configurations, inputs here are natural domain variables (e.g., square footage, temperature, protein properties). The expensive model is a random forest with 1500 trees and the surrogate is a decision tree, with all other settings identical to the main experiments (Section 6.1).

Gate properties. Table 11 reports gate statistics across tolerance levels. Gate AUC is notably lower (≈ 0.52) than on LCBench (≈ 0.58), reflecting that degradation is harder to predict from natural features than from hyperparameter configurations. Despite this, the structural pattern persists: feasibility is driven by the base safe rate π , and coverage increases with τ even under weak gate discrimination.

Guarantee reliability. Table 12 reports the fraction of (dataset, τ) pairs violating the target α . Gate conformal achieves strong guarantee reliability: at $\alpha = 0.1$, zero violations are observed, and at $\alpha \geq 0.2$, violation rates remain well below $\delta = 0.10$. This conservative behavior is expected: the low AUC forces the conformal procedure to select high thresholds, routing fewer but safer inputs. In contrast, regression conformal and naive thresholding violate α at substantially higher rates (32–71%), consistent with the main experiments.

Table 11: Gate properties and conformal routing performance across tolerance levels on 22 general-purpose OpenML datasets. Coverage and violation at $\alpha = 0.2$ averaged over datasets with positive coverage.

τ	π	AUC		Conf. ($\alpha=0.2$)	
		(med.)	ECE	Cov.	Viol.
-1.5	0.18	0.53	0.06	0.000	—
-1.0	0.19	0.52	0.05	0.000	—
0.0	0.43	0.52	0.16	0.048	0.20
0.5	0.69	0.52	0.14	0.452	0.05
1.0	0.73	0.51	0.11	0.462	0.04
2.0	0.77	0.52	0.11	0.557	0.04

Table 12: Fraction of (dataset, τ) pairs where the realized violation rate exceeds target α on general-purpose OpenML datasets. Gate conformal maintains strong safety control. Baselines violate substantially more often.

α	Gate Conf.	Reg. Conf.	Naive
0.10	0/35 (0.0%)	20/62 (32.3%)	64/91 (70.3%)
0.20	1/38 (2.6%)	48/88 (54.5%)	58/91 (63.7%)
0.30	2/43 (4.7%)	50/105 (47.6%)	53/91 (58.2%)
0.50	4/66 (6.1%)	50/112 (44.6%)	39/91 (42.9%)

Summary. The general-purpose OpenML results replicate all main findings: (1) the conformal guarantee holds across α values, with even stronger reliability than on LCBench; (2) feasibility is governed by π rather than absolute AUC; (3) gate conformal dominates regression conformal in guarantee reliability; (4) when gate discrimination is weak (AUC ≈ 0.52), the framework reduces coverage rather than violating safety. These results confirm that the framework generalizes beyond hyperparameter configuration data to diverse real-world regression tasks where inputs are natural domain variables.